Available online at www.sciencedirect.com

ScienceDirect

Ceramics International 40 (2014) 551–555

CERAMICS INTERNATIONAL

www.elsevier.com/locate/ceramint

Photoluminescence properties of $(Sr_{1-x}Ca_x)_{1-y}ZrO_3:yEu^{3+}$ phosphors for near-ultraviolet excited LEDs

K.N. Shinde[a], A. Hakeem[a], S.J. Dhoble[b], K. Park[a,*]

[a]Faculty of Nanotechnology and Advanced Materials Engineering, Sejong University, Seoul 143-747, Republic of Korea
[b]Department of Physics, R.T.M. Nagpur University, Nagpur 440033, India

Received 24 March 2013; received in revised form 12 June 2013; accepted 12 June 2013
Available online 18 June 2013

Abstract

Red-emitting $(Sr_{1-x}Ca_x)_{1-y}ZrO_3:yEu^{3+}$ ($0 \le x \le 1.0$ and $0.01 \le y \le 0.1$) phosphors are synthesized by a modified solid-state reaction. The crystal structure and photoluminescence properties of the $(Sr_{1-x}Ca_x)_{1-y}ZrO_3:yEu^{3+}$ are studied, depending on Ca^{2+} and Eu^{3+} contents. The emission peak (614 nm) from the $^5D_0 \rightarrow {}^7F_2$ transition is much stronger than that (592 nm) from the $^5D_0 \rightarrow {}^7F_1$ transition, indicating efficient red emission. The substitution of Ca^{2+} for Sr^{2+} in $Sr_{0.95}ZrO_3:0.05Eu^{3+}$ greatly enhances the excitation and emission intensities. The most efficient red emission is obtained for the $Ca_{0.95}ZrO_3$:0.05Eu phosphor. The $Ca_{0.95}ZrO_3:0.05Eu^{3+}$ phosphor is a strong candidate as a red component for phosphor-converted white LEDs.

Keywords: A. Sintering; A. Powders: solid state reaction; B. Microstructure-final; C. Optical properties

1. Introduction

Recently, light emitting diodes (LEDs) have been emerged as an important class of source for white light [1]. The commercial red phosphor for near-ultraviolet (NUV) InGaN-based LEDs is trivalent-europium-doped yttrium oxysulfide ($Y_2O_2S:Eu^{3+}$) [1,2]. Yttrium oxysulfide is a wide band gap semiconductor with a bandgap of 4.6–4.8 eV [3]. Many phosphors doped with Eu^{3+} ions can be excited by NUV light at around 400 nm due to the intra-configurational $4f^6$–$4f^6$ transition of Eu^{3+}, and then emit red light, which originates from the $^5D_0$–^7F_j ($j=1$, 2, 3, and 4) transitions of Eu^{3+} [4,5]. The $Y_2O_2S:Eu^{3+}$ phosphor has higher luminous efficiency, better color saturation, and sharper emission lines in comparison with other red phosphors [4]. The high brightness, excellent color definition, and linear response in the wide range of current density of $Y_2O_2S:Eu^{3+}$ are also useful for the manufacture of UV excited devices and the future generation of display equipment [6].

However, the efficiency of the $Y_2O_2S:Eu^{3+}$ red phosphor is about eight times less than that of ZnS:(Cu^+, Al^{3+}) green phosphor and $BaMgAl_{10}O_{17}:Eu^{2+}$ blue phosphor. In addition, its lifetime is inadequate under extended UV irradiation [1]. It suffers from a lack of chemical stability and lifetime [4]. It is therefore necessary to develop new alternative red phosphors that can be effectively excited by the NUV, efficiently emit red light, and have high chemical stability. In recent years, a great deal of attention has been paid to oxide-based luminescent materials due to their high chemical stability and wide range of applications in the lighting industry. The choice of host material and method of preparation for high-performance phosphors are important.

Recently, Eu^{3+} doped alkaline earth zirconates, $SrZrO_3:Eu^{3+}$ and $CaZrO_3:Eu^{3+}$, were reported to have good emission properties [7,8]. Zhang et al. [7] reported that the $SrZrO_3:Eu^{3+}$ phosphor emitted red light under UV light. The luminescence spectra showed small shifts in the position of the emission maxima when excited at different wavelengths due to the different environments for Eu^{3+} in the matrix. In addition, Shimizu et al. [8] reported that Eu^{3+} and Mg^{2+} co-doped $CaZrO_3$ phosphors showed red light emission, regardless of Eu^{3+} content. The Eu^{3+} and Mg^{2+} co-doping in zirconate

*Corresponding author. Tel.: +82 2 3408 3777; fax: +82 2 3408 4342.
E-mail address: kspark@sejong.ac.kr (K. Park).

0272-8842/$ - see front matter © 2013 Elsevier Ltd and Techna Group S.r.l. All rights reserved.
http://dx.doi.org/10.1016/j.ceramint.2013.06.037

substantially enhanced the emission intensity probably due to the increase of the local lattice distortion around the Eu^{3+} ions by Mg^{2+} substitution for Ca^{2+} ions. A combinatorial approach has been used as an effective high-throughput searching tool for multi-component phosphors [9]. It has also been known that luminescent properties can be significantly enhanced when a suitable amount of Eu^{3+} activators is doped to host materials. Therefore, for the first time, we explore $(Sr_{1-x}Ca_x)_{1-y}ZrO_3:yEu^{3+}$ ($0 \le x \le 1.0$ and $0.01 \le y \le 0.1$) red phosphors for white LEDs. The aim of the present work is to investigate the photoluminescence (PL) properties of Eu^{3+} ions doped $(Sr_{1-x}Ca_x)_{1-y}ZrO_3:yEu^{3+}$ phosphors, considering Ca^{2+} and Eu^{3+} contents.

2. Experimental

The $(Sr_{1-x}Ca_x)_{1-y}ZrO_3:yEu^{3+}$ ($0 \le x \le 1.0$ and $0.01 \le y \le 0.1$) phosphors were synthesized by a modified solid-state reaction. $SrCO_3$, $CaCO_3$, ZrO_2, and $(NH_4)_2HPO_4$ powders were used as host materials, and Eu_2O_3 powder was used as an activator. These powders were weighed in proper molar ratio and homogeneously mixed. Subsequently, the mixed powders were ground in mortar. In order to obtain high-purity compounds, two firing steps were used. First, the mixed powders were heated at 500 °C for 4 h in a covered alumina crucible, cooled down to room temperature, and then thoroughly ground in mortar. The firing of the ground powders was conducted at 1300 °C for 9 h in air, thereby yielding white $(Sr_{1-x}Ca_x)_{1-y}ZrO_3:yEu^{3+}$ phosphor powders.

To characterize the crystal structure of the prepared phosphors, an X-ray diffractometer (XRD; Rigaku RINT2000) with Cu Kα radiation ($\lambda = 0.15418$ nm) was used. The morphological characteristics of the phosphors were investigated with a field emission scanning electron microscope (FE-SEM; Hitachi S4700). The ultraviolet PL spectra of the phosphors at room temperature were obtained using a spectrofluorometer (QM-4/2005SE, PTI, USA) with a 75W Xenon lamp. All the PL excitation and emission spectra were obtained with the same amount of phosphors and recorded in the same condition.

3. Results and discussion

Fig. 1(a) and (b) shows the XRD patterns of $Sr_{1-y}ZrO_3:yEu^{3+}$ ($0.01 \le y \le 0.1$) and $Ca_{1-y}ZrO_3:yEu^{3+}$ ($0.01 \le y \le 0.1$) phosphor powders, respectively. The two phosphors crystallize in orthorhombic crystal structure (Pnma). The XRD patterns of the $Sr_{1-y}ZrO_3:yEu^{3+}$ and $Ca_{1-y}ZrO_3:yEu^{3+}$ agree with the JCPDS cards 44-0161 and 35-0790, respectively. The lattice parameters of $SrZrO_3$ are $a = 5.817$ Å, $b = 8.204$ Å, and $c = 5.797$ Å, and those of $CaZrO_3$ are $a = 5.755$ Å, $b = 8.010$ Å and $c = 5.592$ Å. The doped Eu^{3+} has virtually no effect on the crystal structure. For $Sr_{1-y}ZrO_3:yEu^{3+}$ ($0.01 \le y \le 0.1$) powders, in addition to the $Sr_{1-y}Eu_yZrO_3$, a small amount of $Sr_3Zr_2O_7$ with orthorhombic structure (JCPDS cards 30-1319) and ZrO_2 with monoclinic structure (JCPDS cards 37-1484) is detected. Also, $Ca_{1-y}ZrO_3:yEu^{3+}$ ($0.01 \le y \le 0.1$) powders contain a small amount of $CaZr_4O_9$ with orthorhombic structure (JCPDS cards 28-0887), along with the $Ca_{1-y}Eu_yZrO_3$. These impurity phases may be formed by incomplete reaction between the

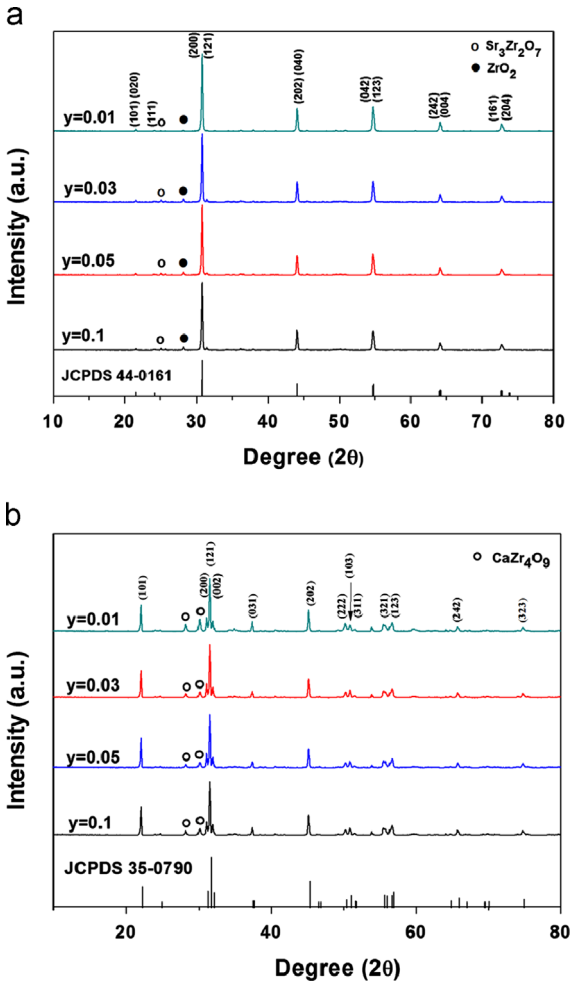

Fig. 1. XRD patterns of the annealed (a) $Sr_{1-y}ZrO_3:yEu^{3+}$ ($0.01 \le y \le 0.1$) and (b) $Ca_{1-y}ZrO_3:yEu^{3+}$ ($0.01 \le y \le 0.1$) phosphor powders.

materials used. The crystallite size (D) of the $Sr_{1-y}ZrO_3:yEu^{3+}$ and $Ca_{1-y}ZrO_3:yEu^{3+}$ phosphors can be calculated from the broadening of a few strong peaks, using Scherrer's formula [10]: $D = (0.9\lambda)/(\beta \cos\theta)$, where λ is the wavelength of radiation ($\lambda = 1.5406$ Å), θ is the angle of the diffraction peak, and β is the full width at half maximum (FWHM) of the diffraction peak (in radian). The average crystallite sizes of the $Sr_{1-y}ZrO_3:yEu^{3+}$ phosphors with $y = 0.01$, 0.03, 0.5, and 1.0 are calculated to be 43, 43, 50, and 48 nm, respectively, and those of the $Ca_{1-y}ZrO_3:yEu^{3+}$ ($0.01 \le y \le 0.1$) phosphors are 54 nm, irrespective of Eu^{3+} content. This means that the annealed phosphors have a nanocrystalline nature.

Fig. 2 represents the XRD patterns of $(Sr_{1-x}Ca_x)_{0.95}ZrO_3:0.05Eu^{3+}$ ($0.2 \le x \le 0.8$) phosphor powders. The primary phases of the complex compounds $(Sr_{1-x}Ca_x)_{0.95}ZrO_3:0.05Eu^{3+}$ are the $Sr_{0.95}Eu_{0.05}ZrO_3$ and $Ca_{0.95}Eu_{0.05}ZrO_3$ with orthorhombic structure. In addition to the $Sr_{0.95}Eu_{0.05}ZrO_3$ and $Ca_{0.95}Eu_{0.05}ZrO_3$ phases, a small amount of orthorhombic $CaZr_4O_9$ (JCPDS cards 28-0887) is observed. With an increase of Ca^{2+} content, the amount of the $Ca_{0.95}Eu_{0.05}ZrO_3$ and $CaZr_4O_9$ phases is increased. No Eu^{3+}-containing compounds are detected. This indicates that the doped Eu^{3+} is present in the complex compound lattice.

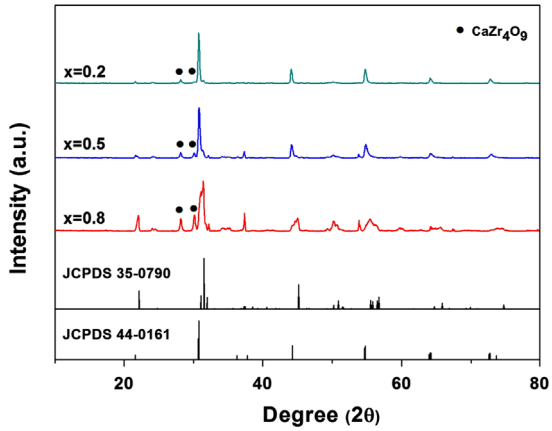

Fig. 2. XRD patterns of the annealed $(Sr_{1-x}Ca_x)ZrO_3$:0.05Eu^{3+} (x=0.2, 0.5, and 0.8) phosphor powders.

The $(Sr_{1-x}Ca_x)_{1-y}ZrO_3$:$yEu^{3+}$ ($0 \le x \le 1.0$ and $0.01 \le y \le 0.1$) phosphor powders, synthesized by the modified solid-state reaction, show excellent morphological characteristics, i.e., a spherical-like shape and smooth surface. These characteristics are favorable for improved PL properties [11]. All the powders possess nearly the same morphology and size, irrespective of the Ca^{2+} and Eu^{3+} contents. Agglomeration in some powders and a slight change in their surface morphology are found. For example, FE-SEM images of the $Ca_{0.95}ZrO_3$:0.05Eu^{3+}, $Sr_{0.95}ZrO_3$:0.05Eu^{3+}, and $(Sr_{0.2}Ca_{0.8})_{0.95}ZrO_3$:0.05$Eu^{3+}$ phosphor powders are shown in Fig. 3.

Fig. 4 exhibits the excitation spectra of $(Sr_{1-x}Ca_x)_{0.95}ZrO_3$:0.05$Eu^{3+}$ ($0 \le x \le 1.0$) phosphors. The excitation spectra are obtained in 350–450 nm wavelengths by monitoring the $^5D_0 \rightarrow {}^7F_2$ transition of Eu^{3+} at 614 nm. An intense peak is located at 393 nm, which is caused by the characteristic $^7F_0 \rightarrow {}^5L_6$ transition of Eu^{3+} [4]. Other excitation peaks centered at 364, 384, and 418 nm correspond to the $^7F_0 \rightarrow {}^5D_4$, $^7F_0 \rightarrow {}^5G_2$, and $^7F_0 \rightarrow {}^5D_3$ transitions of Eu^{3+}, respectively [4]. Clearly, the most efficient excitation at 393 nm means that these phosphors can be effectively excited by NUV. The excitation intensity is increased with an increase in Ca^{2+} content up to x=1.0.

Fig. 5 shows the emission spectra of $(Sr_{1-x}Ca_x)_{0.95}ZrO_3$:0.05$Eu^{3+}$ ($0 \le x \le 1.0$) phosphors under excitation at 393 nm. The strong emission peaks are located at 592 and 614 nm, which are due to the $^5D_0 \rightarrow {}^7F_1$ and $^5D_0 \rightarrow {}^7F_2$ transitions of Eu^{3+}, respectively [12,13]. The emission peak (592 nm) from the $^5D_0 \rightarrow {}^7F_1$ transition is much weaker than that (614 nm) from the $^5D_0 \rightarrow {}^7F_2$ transition. This indicates that the $(Sr_{1-x}Ca_x)_{0.95}ZrO_3$:0.05$Eu^{3+}$ phosphors have efficient red emission characteristics. The $^5D_0 \rightarrow {}^7F_2$ and $^5D_0 \rightarrow {}^7F_1$ transitions offer red and orange lights, respectively. In addition to the two strong peaks, a very weak peak centered at 554 nm is observed, which is caused by the $^5D_1 \rightarrow {}^7F_2$ transition of Eu^{3+} [14,15]. The intensity of transitions between different j-number levels in the $^5D_0 \rightarrow {}^7F_j$ (j=1 and 2) transition is dependent upon the symmetry of the local environment of the Eu^{3+} ion. When the Eu^{3+} is located at a low-symmetry local site without an inversion center, the emission caused by the $^5D_0 \rightarrow {}^7F_2$ transition is dominated in the emission spectra [16]. The introduction of Ca^{2+} into the $Sr_{0.95}ZrO_3$ lattice results in a lower symmetry of the Eu^{3+} ion site and thus a hypersensitive transition of the Eu^{3+} ion. Here, the $^5D_0 \rightarrow {}^7F_1$ and $^5D_0 \rightarrow {}^7F_2$ transitions of Eu^{3+} are split into three and five components, respectively [17]. The intensity of transitions between different j-number levels in the $^5D_0 \rightarrow {}^7F_j$ (j=1 and 2) transition can be described in terms of the Judd–Ofelt theory [18]. Each level can be split into up to $2j$+1 sublevels (j=1 and 2 in this case) by the local crystal field surrounding the Eu^{3+} ion. As shown in the inset to Fig. 5, the emission intensity is increased with an increase in Ca^{2+} content up to x=1.0.

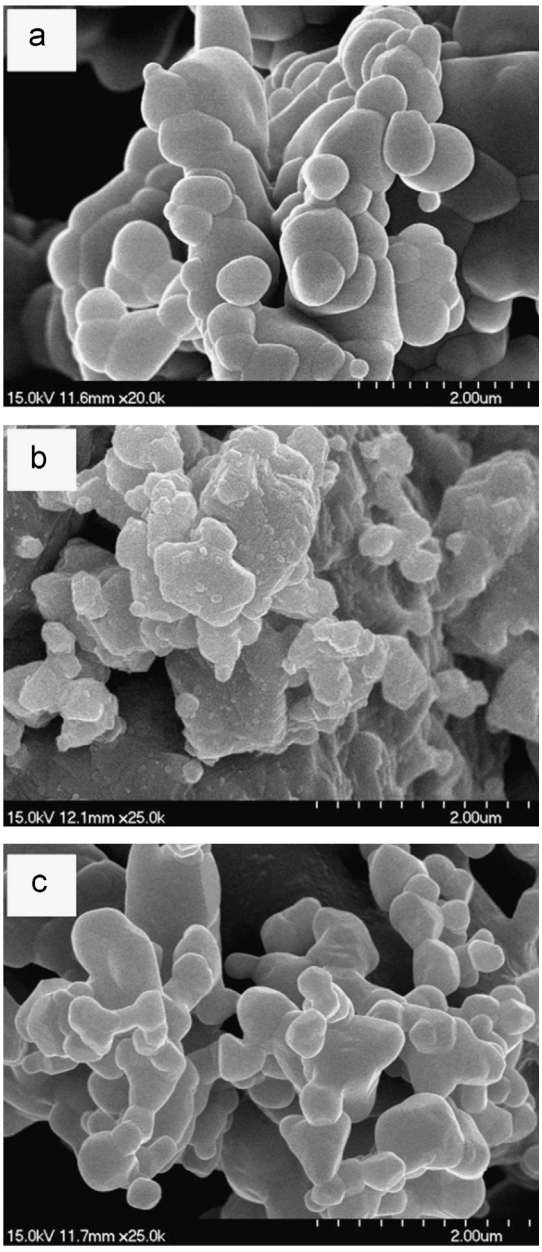

Fig. 3. FE-SEM images of (a) $Ca_{0.95}ZrO_3$:0.05Eu^{3+}, (b) $Sr_{0.95}ZrO_3$:0.05Eu^{3+}, and (c) $(Sr_{0.2}Ca_{0.8})_{0.95}ZrO_3$:0.05$Eu^{3+}$ phosphor powders.

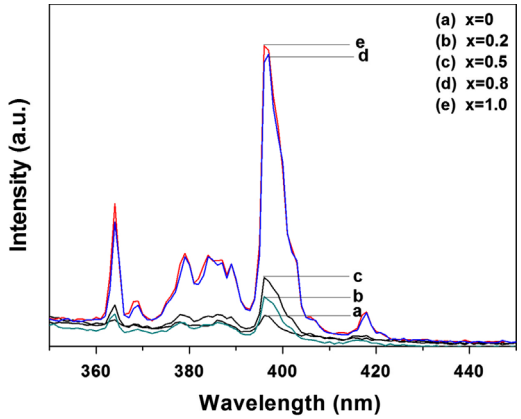

Fig. 4. Excitation spectra of $(Sr_{1-x}Ca_x)_{0.95}ZrO_3:0.05Eu^{3+}$ ($0 \le x \le 1.0$) phosphors.

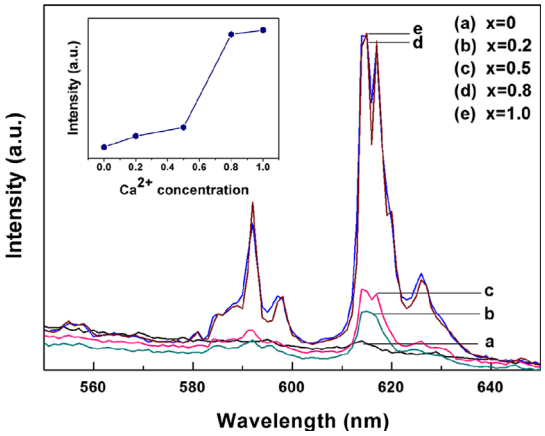

Fig. 5. Emission spectra of $(Sr_{1-x}Ca_x)_{0.95}ZrO_3:0.05Eu^{3+}$ ($0 \le x \le 1.0$) phosphors.

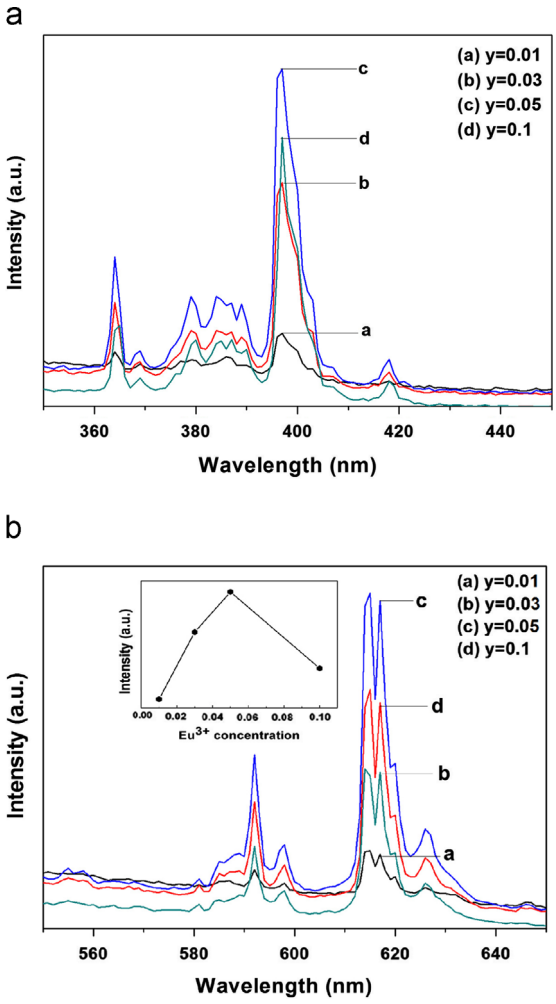

Fig. 6. (a) Excitation and (b) emission spectra of $Ca_{1-y}ZrO_3:yEu^{3+}$ ($0.01 \le y \le 0.1$) phosphors.

To further improve the PL characteristics, we fabricated $Ca_{1-y}ZrO_3:yEu^{3+}$ ($0.01 \le y \le 0.1$) phosphors with various Eu^{3+} contents. The Eu^{3+} content is one of the most important factors influencing the performance of the phosphors [4,5]. It is thus necessary to find out the optimum Eu^{3+} content. Fig. 6(a) and (b) shows the excitation and emission spectra of $Ca_{1-y}ZrO_3:yEu^{3+}$ ($0.01 \le y \le 0.1$) phosphors with various Eu^{3+} contents, respectively. The excitation and emission characteristics of the $Ca_{1-y}ZrO_3:yEu^{3+}$ phosphors are nearly the same as those of the $(Sr_{1-x}Ca_x)_{0.95}ZrO_3:0.05Eu^{3+}$ phosphors, except their intensity. The excitation and emission intensities increase with an increase of Eu^{3+} content up to $y=0.05$ and then decrease slightly by further increasing the Eu^{3+} content. The decrease is primarily because the energy absorbed by Eu^{3+} is released as a non-radiation transition instead of a red light emission [19]. The PL properties of $(Sr_{1-x}Ca_x)_{1-y}ZrO_3:yEu^{3+}$ phosphors depend strongly on Ca^{2+} and Eu^{3+} contents. The $Ca_{0.95}ZrO_3:0.05Eu^{3+}$ phosphor shows the most efficient red emission.

4. Conclusions

All the $(Sr_{1-x}Ca_x)_{1-y}ZrO_3:yEu^{3+}$ ($0 \le x \le 1.0$ and $0.01 \le y \le 0.1$) phosphor powders were crystallized in the orthorhombic structure. The $(Sr_{1-x}Ca_x)_{1-y}ZrO_3:yEu^{3+}$ phosphor powders, synthesized by the modified solid-state reaction method, showed excellent morphological characteristics, i.e., spherical-like shape and smooth surface. The strongest excitation peak was observed at 393 nm, which was caused by the characteristic $^7F_0 \rightarrow {}^5L_6$ transition of Eu^{3+}. The strong emission peaks were located at 592 and 614 nm, which were attributed to the $^5D_0 \rightarrow {}^7F_1$ and $^5D_0 \rightarrow {}^7F_2$ transitions of Eu^{3+}, respectively. The excitation and emission intensities of the $(Sr_{1-x}Ca_x)_{0.95}ZrO_3:0.05Eu^{3+}$ phosphors increased with an increase in the Ca^{2+} content up to $x=1.0$. Among the $(Sr_{1-x}Ca_x)_{1-y}ZrO_3:yEu^{3+}$ phosphors, the $Ca_{0.95}ZrO_3:0.05Eu^{3+}$ phosphor showed excellent PL characteristics and could be a strong candidate as a red component for white LEDs.

References

[1] S. Neeraj, A.K. Kijima, A.K. Cheetham, Novel red phosphors for solid-state lighting: the system $NaM(WO_4)_{2-x}(MoO_4)_x:Eu^{3+}$ (M=Gd, Y, Bi), Chemical Physics Letters 387 (2004) 2–6.

[2] T.W. Chou, S. Mylswamy, R.S. Liu, S.Z. Chuang, Eu substitution and particle size control of Y_2O_2S for the excitation by UV light emitting diodes, Solid State Communications 136 (2005) 205–209.

[3] J. Thirumalai, R. Jagannathan, D.C. Trivedi, $Y_2O_2S:Eu^{3+}$ nanocrystals, a strong quantum-confined luminescent system, Journal of Luminescence 126 (2007) 353–358.

[4] B. Han, J. Zhang, Q. Cui, Y. Liu, A potential reddish orange emitting phosphor $Ca_2BO_3Cl:Eu^{3+}$ for white light-emitting diodes, Physica B 407 (2012) 3484–3486.
[5] Y.R. Shi, Z.G. Yang, W.J. Wang, G. Zhu, Y.H. Wang, Novel red phosphors $Na_2CaSiO4:Eu^{3+}$ for light-emitting diodes, Materials Research Bulletin 46 (2011) 1148–1150.
[6] Z. Fu, Y. Geng, H. Chen, S. Zhou, H.K. Yang, J.H. Jeong, Combustion synthesis and luminescent properties of the Eu^{3+}-doped yttrium oxysulfide nanocrystalline, Optical Materials 31 (2008) 58–62.
[7] A. Zhang, M. Lu, G. Zhou, Y. Zhou, Z. Qiu, Q. Ma, Synthesis, characterization and luminescence of Eu^{3+}-doped $SrZrO_3$ nanocrystals, Journal of Alloys and Compounds 468 (2009) L17–L20.
[8] Y. Shimizu, S. Sakagami, K. Goto, Y. Nakachi, K. Ueda, Tricolor luminescence in rare earth doped $CaZrO_3$ perovskite oxides, Materials Science and Engineering B 161 (2009) 100–103.
[9] K.Y. Jung, Luminescence optimization of $MBO_3:Eu^{3+}$ (M=Y, Gd, Al) red phosphor by spray pyrolysis using combinatorial chemistry, Physica B 405 (2010) 3195–3199.
[10] K. Park, M.H. Heo, K.Y. Kim, S.J. Dhoble, Y. Kim, J.Y. Kim, Powder Technology 237 (2013) 102–106.
[11] X. Xiao, B. Yan, Chemical co-precipitation synthesis and photoluminescence of Eu^{3+} or Dy^{3+} doped $Zn_3Nb_2O_8$ microcrystalline phosphors from hybrid precursors, Materials Science and Engineering B 136 (2007) 154–158.
[12] K. Park, K.Y. Kim, Synthesis and photoluminescence of nano-sized (Gd, Y)$PO_4:Eu^{3+}$ by solution combustion method, Journal of Nanoscience and Nanotechnology 11 (2011) 7361–7364.
[13] K. Park, S.W. Nam, M.H. Heo, VUV photoluminescece properties of $Y_{1-x}Gd_xVO_4$:Eu phosphors prepared by ultrasonic spray pyrolysis, Ceramics International 36 (2010) 1541–1544.
[14] A.G. Joly, W. Chen, J. Zhang, S. Wang, Electronic energy relaxation and luminescence decay dynamics of Eu^{3+} in $Zn_2SiO_4:Eu^{3+}$ phosphors, Journal of Luminescence 126 (2007) 491–496.
[15] J. Zhao, C. Guo, J. Yu, R. Yu, Spectroscopy properties of Eu^{3+} doped $Ca_9R(VO_4)_7$ (R=Bi, La, Gd and Y) phosphors by sol–gel method, Optics and Laser Technology 45 (2013) 62–68.
[16] X. Su, B. Yan, H. Huang, In situ co-precipitation synthesis and luminescence of $GdVO_4$: Eu^{3+} and $Y_xGd_{1-x}VO_4$: Eu^{3+} microcrystalline phosphors derived from the assembly of hybrid precursors, Journal of Alloys and Compounds 399 (2005) 251–255.
[17] B.N. Mahalley, S.J. Dhoble, R.B. Pode, G. Alexander, Photoluminescence in $GdVO_4:Bi^{3+}$, Eu^{3+} red phosphor, Applied Physics A 70 (2000) 39–45.
[18] H. Meyssamy, K. Riwotzki, A. Kornowski, S. Naused, M. Haase, Wet-chemical synthesis of doped colloidal nanomaterials: particles and fibers of $LaPO_4$:Eu, $LaPO_4$:Ce, and $LaPO_4$:Ce,Tb, Advanced Materials 11 (1999) 840–844.
[19] D.L. Dexter, Theory of concentration quenching in inorganic phosphors, Journal of Chemical Physics 22 (1954) 1063–1071.